SCIENTIFIC REPORTS

SUBJECT AREAS:
MAGNETIC PROPERTIES AND MATERIALS
SURFACES, INTERFACES AND THIN FILMS
APPLIED PHYSICS
SPINTRONICS

Received
2 October 2012

Accepted
26 November 2012

Published
21 January 2013

Correspondence and requests for materials should be addressed to T.W. (tomwu@ntu.edu.sg)

Anomalous exchange bias at collinear/noncollinear spin interface

Y. F. Tian[1], J. F. Ding[1], W. N. Lin[1], Z. H. Chen[2], A. David[1], M. He[1], W. J. Hu[1], L. Chen[2] & T. Wu[1]

[1]Division of Physics and Applied Physics, School of Physical and Mathematical Sciences, Nanyang Technological University, Singapore 637371, Singapore, [2]School of Materials Science and Engineering, Nanyang Technological University, Singapore, 639798, Singapore.

We report on the interfacial magnetic coupling in manganite bilayers of collinear ferromagnetic $La_{0.7}Sr_{0.3}MnO_3$ and noncollinear multiferroic $TbMnO_3$. Exchange bias is observed at the Néel temperature of $TbMnO_3$ (~41 K) due to the onset of long-range antiferromagnetic ordering in the Mn spin sublattice. Interestingly, an anomalous plateau of exchange bias emerges at the ordering temperature of Tb spins (~10 K), and we ascribe this unique feature to the strong coupling between Tb and Mn spin sublattices in $TbMnO_3$, which in turn influences the magnetic coupling across the interface. On the other hand, the enhancement of coercivity in $La_{0.7}Sr_{0.3}MnO_3/TbMnO_3$ shows monotonous temperature dependence. Our results illustrate a strong interfacial magnetic interaction at the $La_{0.7}Sr_{0.3}MnO_3/TbMnO_3$ interface, highlighting the roles of competing spin orders, magnetic frustration, and coupling between multiple spin sublattices in artificial collinear/noncollinear spin heterostructures.

Interfaces of transition metal oxides are promising to offer fascinating physical properties because of the strong correlations between charge, spin, orbital and lattice degrees of freedom[1]. In oxide heterostructures, novel electrical and magnetic ground states may emerge as a result of charge transfer, electronic and orbital reconstruction, which has attracted increasing attention[2–5]. Particularly, multiferroic materials simultaneously exhibit at least two types of ferroic or antiferroic orders[6–11], and the coupling between ferroelectric and magnetic orders facilitates the interconversion of electric and magnetic energies which may find novel applications in memory and logic devices[12–15]. Recently, exchange bias (EB), which was originally discovered in bilayers of ferromagnetic (FM) and antiferromagnetic (AFM) materials as a result of the magnetic coupling and pinning effects at interface[16–20], was observed in multiferroic $BiFeO_3$ (BFO) heterostructures[13,21–27]. Such multiferroic heterostructures with EB represents a milestone on the path towards next generation magnetoelectric devices[27]. However, although the EB effect, which is characterized by a shift in the magnetization loops away from the zero field axis, was discovered half a century ago and has found important technological applications in data storage and magnetoresistive sensors, its microscopic origin has not yet been fully elucidated. For instance, the issues regarding the coupling configurations at the interface[28,29] and the correlations between exchange bias field (H_E), coercivity (H_C) and interfacial exchange coupling[30–32] are under a lot of debate. In the past decades, EB effect in magnetic heterostructures has remained as an active research area, and there have been reports on EB effect in a myriad of oxide bilayers and supperlattices[33–38]. Incorporating multiferroic oxides into such oxide heterostructures adds a new dimension to the EB research and offers exciting opportunities.

In this work, we focus on the magnetic coupling between a multiferroic $TbMnO_3$ (TMO) with noncollinear spin order and a prototypical collinear ferromagnet $La_{0.7}Sr_{0.3}MnO_3$ (LSMO). To the best of our knowledge, this is the first study on the magnetic interaction at a collinear/noncollinear spin heterointerface. TMO is a perovskite-structured multiferroic with a frustrated spiral spin order, exhibiting intricate magnetoelectric and magnetocapacitance effects[39–46]. The Mn sublattice in TMO single crystals shows a sinusoidal spin order along the *b* axis at the Néel temperature $T_N \sim 41$ K (Fig. 1(a)), and the spin order becomes spiral (Fig. 1(b)) in the *bc* plane at the ferroelectric transition temperature $T_{lock} \sim 28$ K. The broken inversion symmetry due to the noncollinear magnetic structure leads to the formation of a ferroelectric polarization along the *c* direction[39–43]. Upon decreasing temperature, the Tb^{3+} ions show a long-range spin ordering at $T_{Tb} \sim 7$ K (schematically shown in Fig. 1(b))[39,43,46]. We should note here that there have been only a few reports on the magnetic order in TMO at $T < 7$ K[39,43,46], and the multiple high-order reflection peaks detected in a recent neutron diffraction study suggest that the order of the Tb spins and their coupling with the Mn spins can be much more complex than the simplified schematic in Fig. 1(b). In particular, neutron scattering and x-ray resonance scattering studies have confirmed the existence of a strong coupling between Tb and Mn ions via the spin-polarized 5*d* conduction band[44–46], and their states are

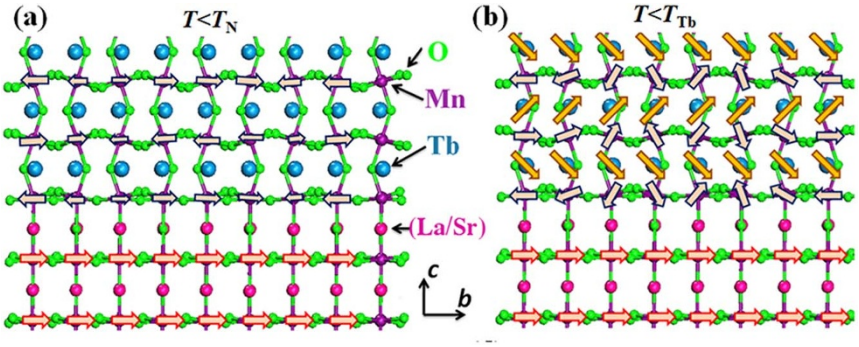

Figure 1 | Schematics of possible spin configurations of the LSMO/TMO interface at the temperature just below Néel temperature T_N (a) and below the Tb spin ordering temperature T_{Tb} (b). Note that these schematics only serve the purpose of illustration and do not represent the exact spin orders at interface.

hybridized. In such noncollinear multiferroics, the complex spin orders and the exchange interactions are important for not only the multiferroic ground states but also potentially provide novel electronic paths towards controlling the magnetic degree of freedom in heterostructures[47–49].

So far, most works on TMO have focused on the properties of bulks and thin films[39,50,51], and the properties of TMO-based heterostructures were seldom studied. Recently, it was demonstrated that rectifying junctions can be formed by growing TMO thin films on conducting Nb-doped $SrTiO_3$ substrates[52,53], but the study was limited to transport properties. In general, there is a lack of effort on incorporating multiferroics with noncollinear spin orders like TMO into functional thin film heterostructures. It has been proposed that the magnetic frustration and the noncollinear spin structure in the AFM layer contribute to the EB effect at the AFM/FM interface[32,54]. Multiferroic TMO exhibits unique and complex spin orders, thus offering new perspectives to exploit the exchange coupling in multiferroic heterostructures. In the LSMO/TMO bilayer illustrated in Fig. 1(a), both Mn and Tb spin sublattices in TMO may couple, either directly or indirectly, with the Mn spin lattice in LSMO. In such a case, we expect to observe not only the onset of EB below the Néel temperature of TMO (Fig. 1(a)), but also additional features in the interfacial magnetic coupling at the ordering temperature of Tb spins (Fig. 1(b)). Such an exchange coupling at the oxide interface highlights the intricate interactions between the multiple spin sublattices, enriching the magnetic properties of multiferroic heterostructures.

Results

Figure 2(a) shows the oscillation of the *in-site* RHEED specular intensity recorded during the growth of bilayer. A layer-by-layer growth mode can be observed for the eight unit cells of LSMO and the first several unit cells of TMO. In addition, as shown in Figure 2(b), the atomic force microscopy (AFM) image measured on the LSMO layer shows a clear step-and-terrace surface with the height of steps being around one unit cell, which is consist with the layer-by-layer growth mode of LSMO. As shown in the XRD θ–2θ scan (Fig. 2(c)), only reflections corresponding to the substrates and the TMO (001) planes were observed, indicating that the films were

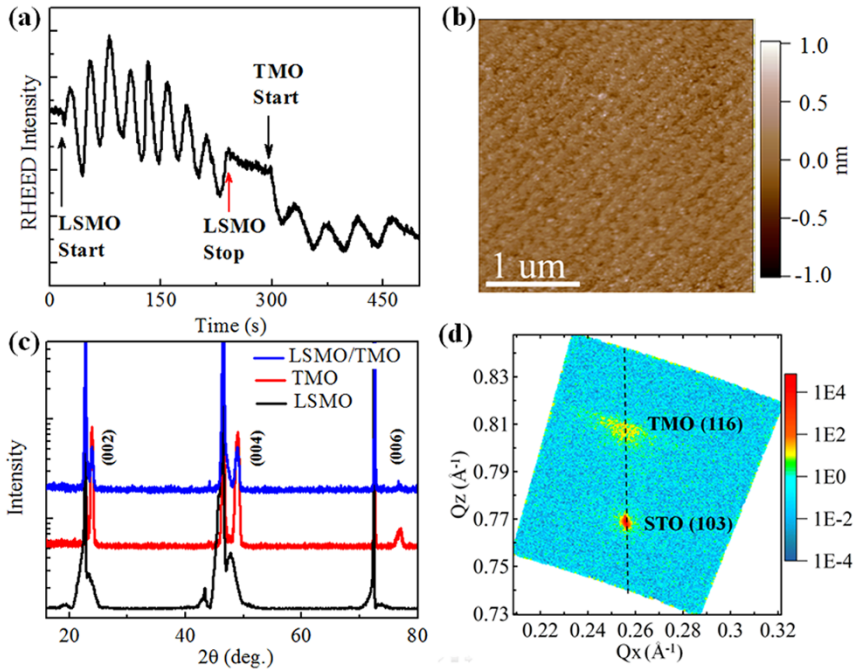

Figure 2 | (a) Intensity oscillation of the *in-site* RHEED recorded during the growth of LSMO/TMO bilayer. (b) AFM image taken after the growth of eight unit cell LSMO layer. (c) XRD θ–2θ data for the LSMO/TMO bilayer and the corresponding reference single layers. Cu-Kα radiation was used to measure the bilayer and the TMO single layer, whereas synchrotron was used to measure the ultrathin LSMO single layer. (d) RSM data around the (103) Bragg reflection of STO measured on the TMO reference single layer. Dashed line is guide to eyes.

c-axis oriented. Because of the ultrathin nature of the LSMO layer, we used synchrotron in the measurements. The XRD data of the reference LSMO single layer shows clear fringes, indicating a high crystalline quality, and the lattice constant of LSMO can be calculated as 3.811±0.05 Å. The compression in the out-of-plane direction is expected since the lattice constant of LSMO (rhombohedral perovskite bulk structure, pseudocubic a=3.873 Å) is smaller than that of STO (cubic, a=3.905 Å). Figure 2(d) further shows the reciprocal space mapping (RSM) data collected around the STO (103) for the TMO reference film. The RSM data clearly reveals that the in-plane lattice parameter of TMO is identical to that of STO, indicating that the films are coherently grown on the substrate and slightly compressively strained[55,56].

Figure 3(a) shows the zero field cooling (ZFC) and field cooling (FC) data of magnetization versus temperature measured on the reference single layer TMO sample. The magnetization shows an upturn at low temperature as a result of the ordering of Mn spins. In the plot of inverse susceptibility (χ^{-1}) vs. temperature, a deviation from the paramagnetic linear behavior occurs at T_N ~ 41 K. On decreasing temperature, the cusp feature at ~10 K can be related to the long range Tb spin ordering (T_{Tb})[39,43,46].

Furthermore, we measured the thermal remanent magnetization after ZFC (RM-ZFC) and FC (RM-FC), which often gives valuable information regarding the irreversible magnetization in disordered systems[57]. During the RM-ZFC (RM-FC) measurements, sample was first cooled down under zero field (6 Tesla) from 300 K, then a 6 Tesla field is applied and removed, which was followed by magnetization measurements under zero field on increasing temperature. As shown in Fig. 3(b), in addition to the magnetic transitions mentioned above, there is a weak anomalous feature at ~26 K in the difference of the ZFC and FC data, which is close to the Mn spiral spin ordering temperature observed in bulk TMO (T_{lock}) at ~28 K, but it is much less pronounced than the bulk result[39].

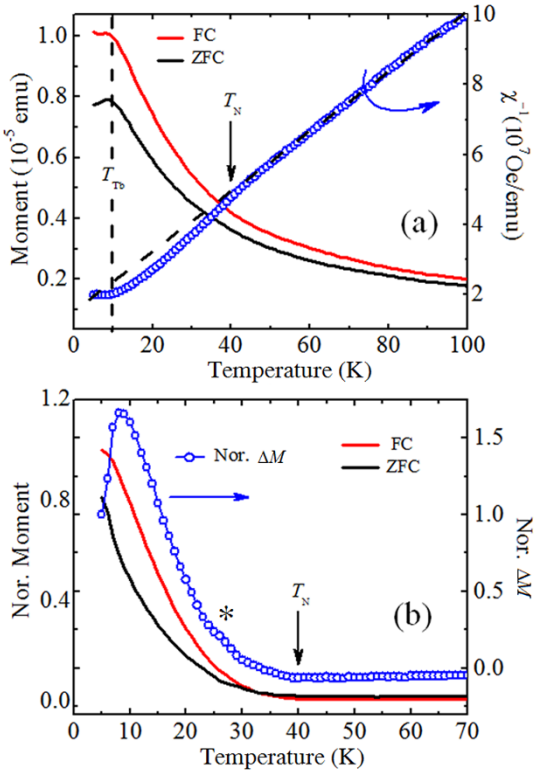

Figure 3 | (a) Low temperature ZFC and FC curves measured on the reference TMO single layer. The magnetic field applied during the measurement is 200 Oe. Also shown is the inverse susceptibility (χ^{-1}) of the FC curve. Dashed lines are guides to the eyes. (b) Temperature dependence of the remanent magnetization measured under the ZFC and FC conditions. The data were normalized according to the value of the FC magnetization at 5 K. Also shown is the difference (ΔM) between the ZFC and FC data. The weak anomalous feature at ~26 K (*) presumably is related to the onset of the spiral spin structure.

Figure 4 shows the ZFC and FC curves and the *M-H* loops measured on the LSMO/TMO bilayer and reference samples. The bifurcation between the ZFC and FC curves which was already observed in the TMO single layer (Fig. 3(a)) becomes stronger in the bilayer (Fig. 4(a)), which likely indicates the magnetic frustration at the LSMO/TMO interface[58]. It was previously proposed that the strain effect can induce a weak ferromagnetic signal at low temperatures[55,59], which was observed in the TMO reference single layer. This weak ferromagnetism of TMO may contribute to the overall magnetism of the LSMO/TMO bilayer. Regarding to the LSMO component, as shown in Fig. 4(a), the Curie temperature of the reference LSMO single layer is ~220 K, which is much lower than the bulk value ~ 369 K. The strong suppression of magnetic properties is likely the result of stain which is known to induce distortion of MnO_6 octahedra in the Jahn-Teller systems[60,61]. In the bilayer, the Curie temperature of LSMO is further suppressed to ~165 K, which indicates that the magnetism of the 8 unit cell LSMO is significantly affected by the presence of the TMO overlayer. We note that the possible intermixing at the LSMO/TMO interface must be limited to one or two unit cells because the Curie temperature of five unit cell LSMO was reported to drastically decease to ~100 K[62]. However, the exact origin of the Curie temperature reduction in the bilayer and the detailed structure of the interface clearly warrant further studies.

The definite evidence of magnetic coupling at the LSMO/TMO interface is the enhancement of coercivity in the bilayer. As shown in Fig. 4(b), at 50 K, H_C of the bilayer is enhanced to 178 Oe, which is much larger than the value of the reference LSMO single layer (44 Oe). Further enhancement was observed at lower temperatures: at 10 K H_C of the bilayer reaches as high as 960 Oe (Fig. 4(c)). Furthermore, we observed the EB effect in the bilayer as evidenced by the shift of the hysteresis loop towards the opposite direction of the cooling field (Fig. 4(d)); H_E at 5 K under a cooling field of 4 Tesla is 42 Oe. The observed exchange coupling and bias unambiguously suggest the existence of interfacial magnetic coupling between LSMO and TMO.

The temperature dependence of H_C and H_E shown in Fig. 5 sheds more light on the magnetic coupling at LSMO/TMO interface. As the temperature goes down, the EB emerges at the Néel temperature T_N of TMO (Fig. 5(a)), which is expected because the AFM order in the TMO layer needs to develop and pin the FM domains of the LSMO layer. However, the magnetic order in TMO is quite complex: besides the A-type and G-type modulated structures, a neutron diffraction study revealed the coexistence of C-type and F-type orderings below T_N[46]. On further decreasing temperature, H_E shows an anomalous plateau around T_{Tb}, and then it increases by almost four fold to a value of 128 Oe. This non-monotonous temperature dependence of H_E reflects the complex magnetic interactions between various spin sublattices. It was proposed that the competing exchange interactions, *i.e.*, magnetic couplings between nearest (J_1) and next nearest (J_2) Mn spin sublattices, along with the clamping magnetic interaction between Tb and Mn (J_{Tb-Mn}) spin sublattices, collectively determine the Mn–O–Mn bound angles and modulate the strength of the exchange interaction between Mn ions in TMO[45]. As a result of the strong coupling between Tb and Mn spin sublattices of TMO[44–46], the formation of long-range Tb^{3+} spin ordering could lead to a significant canting of the neighboring Mn spin order. Consequently, the spin frustration within the AFM TMO layer affects the coupling strength across the interface between the Mn sublattices of TMO and LSMO, resulting in the nontrivial temperature-dependent variation of H_E.

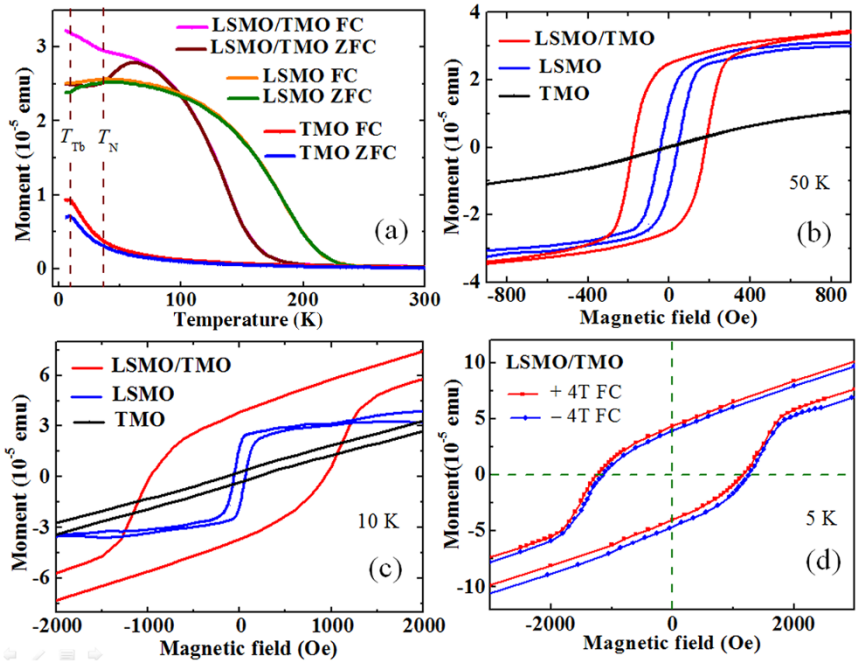

Figure 4 | (a) ZFC and FC data measured on the LSMO/TMO bilayer and reference single layer samples. The applied magnetic field during measurements is 200 Oe. (b) and (c) show the corresponding magnetic hysteresis loops measured at 50 K and 10 K, respectively. The measurements follow a FC procedure from 300 K under a magnetic field of +4 Tesla. (d) Hysteresis loops measured at 5 K on the LSMO/TMO bilayer after the +4/−4 Tesla FC procedure.

However, it is noteworthy that the schematic in Fig. 1(b) apparently over-simplifies the spin configuration at the LSMO/TMO interface. There remain open questions regarding the magnetic ordering of Tb spins in TMO at low temperatures as well as the exchange interactions between the Tb and Mn sublattices[43,44]. Furthermore, although in the schematics of Fig. 1(a) and (b) the MnO_2 layer at the LSMO/TMO interface adopts the spin order of TMO, it is apparently shared by both layers, and spin-flop coupling may develop at the interface[31]. The detailed elucidation may require neutron and synchrotron experiments. As far as we know, there has been no theory so far on elucidating the magnetic order/disorder at such an interface between a spiral multiferroic and a ferromagnet. The anomalous temperature dependence of EB at T_{Tb} invites future theoretical efforts to shed light on the ground-state spin configuration and exchange coupling at such strongly frustrated interfaces.

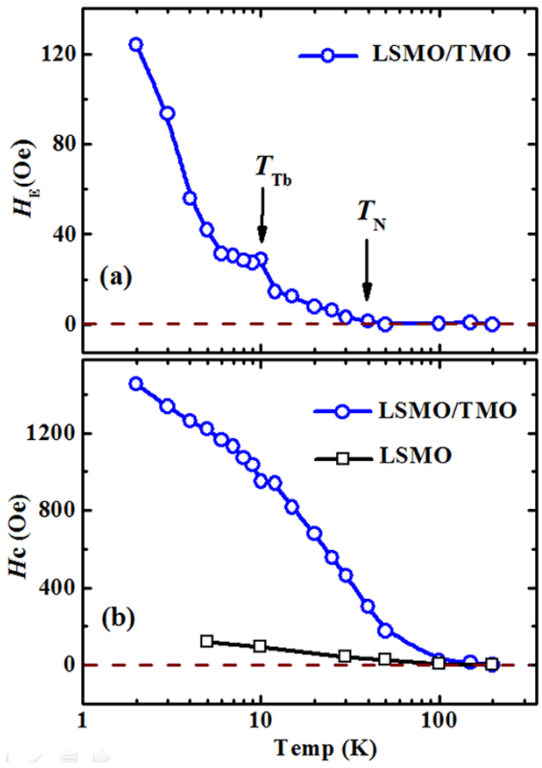

Figure 5 | **Temperature dependence of the exchange bias H_E (a) and the coercivity Hc (b) measured on the LSMO/TMO bilayer.** For comparison, the H_C data of a reference LSMO single layer are also shown.

As shown in Fig. 5(b), the temperature dependence of H_C shows a monotonous behavior, which is different from the trend of H_E, suggesting that H_E and H_C perhaps have different origins. As reported previously, the enhancement of H_C may occur without the onset of H_E, which depends on not only the spin structure in the AFM layer (e.g., collinear or noncollinear) but also the detailed domain structures[54]. The frustration of interfacial spins and the spin-flop coupling between FM and AFM layers have been proposed to be responsible for a large uniaxial anisotropy and enhanced H_C, whereas additional effects like interfacial defects are needed to explain the EB[31,32]. Moreover, because H_C is not an intrinsic property of material, it is sensitively dependent on sample morphology[63] and other factors.

The coercivity is supposed to have a power law dependence on the thickness of FM layer, i.e., $Hc \sim 1/t_{FM}^n$, when the random interaction at the AFM/FM interface is assumed[63]. We measured bilayers with the thickness of LSMO layer varying from 8 to 13 unit cells while keeping the thickness of TMO layer fixed. Indeed, as shown in Fig. 6, both H_C and H_E decrease with increasing LSMO thickness. The enhancement of H_C is quite significant within the range of LSMO layer thickness. In a phenomenological model, the exchange bias field is expressed as $H_E = \Delta\sigma/M_{FM}t_{FM}$, where $\Delta\sigma$ is the interfacial exchange energy density, which represents the strength of interfacial exchange coupling, M_{FM} and t_{FM} are the magnetization and thickness of the FM layer, respectively[16,17]. As show in Fig. 6, H_E appears to follow the trend of $1/t_{FM}$, which is consistent with the interfacial nature of the EB effect.

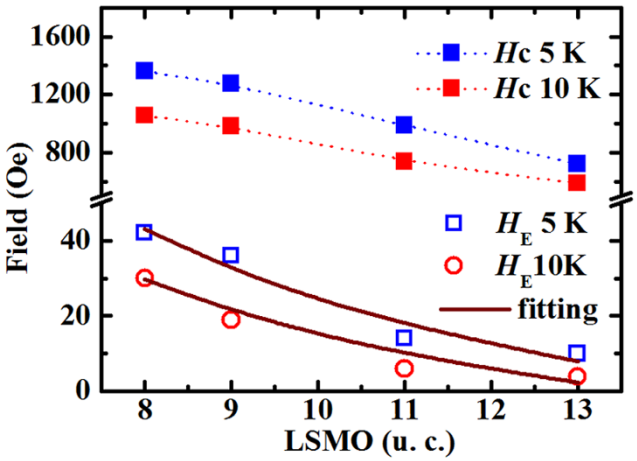

Figure 6 | The dependence of H_E and Hc on the thickness of LSMO, while the thickness of TMO is fixed at 40 nm. Dashed lines are guides to eyes. Solid lines are theoretical fittings to $1/t_{FM}$.

Discussion

As mentioned previously, EB has also been reported in heterostructures made of another multiferroic material BFO, which has attracted lots of attention[4,21,27]. In the previously reported bilayers composed of LSMO (2–10 nm) and BFO (600 nm), an EB shift as high as 225 Oe was observed[27]. A large H_E suggests a high interfacial exchange energy density at the LSMO/BFO interface. On the other hand, the enhancement of Hc is more significant in our LSMO/TMO sample; the largest measured Hc is 1455 Oe, whereas it is about 750 Oe in the LSMO/BFO bilayer reported in reference 27. But we should note here that before utilizing the magnetoelectric properties of TMO in novel devices, the domain structures of TMO must be elucidated, which not only affects the polarization[64,65], but also plays a critical role in the EB effect[16,17,24,27]. However, information on the domain structures of TMO is very limited[56]. Further studies focused on controlling the domain characteristics of TMO thin films through rational synthesis and local probing are needed to tailor the interface properties of TMO-based heterostructures.

In summary, the pronounced EB and the enhancement of coercivity in LSMO/TMO bilayer confirm the existence of a strong interfacial exchange coupling, which is related to the presence of uncompensated spins at the interface between AFM TMO and FM LSMO. The emerging coupling between the Mn and Tb spin sublattices in TMO frustrates the interfacial magnetic coupling in the collinear/noncollinear spin bilayers, leading to the anomalous plateau-like feature of H_E at T_{Tb}. These data put constraints on future theoretical attempts of capturing the complex magnetic coupling in TMO and its heterostructures. Future experimental efforts using interface sensitive synchrotron and neutron probes are imperative to reveal the spin configurations and the domain structures in the vicinity of the LSMO/TMO interface. As the first study on the magnetic properties of such collinear/noncollinear magnetic heterostructures, our results also invite theoretical investigations on the exchange coupling at oxide interfaces involving noncollinear and frustrated spin structures. We can envisage that further elucidation of the coupling between multiple spin lattices will open new avenues towards manipulating the ferroic orders in oxide heterostructures.

Methods

We prepared thin film bilayers of LSMO/TMO on TiO_2-terminated $SrTiO_3$ (001) single crystal substrates at 750°C using pulsed laser deposition. The frequency of the excimer laser was 1 Hz and 2 Hz for LSMO and TMO, respectively. A laser fluence of ~1.5 J/cm^2 was calibrated and used for the depositions. The growth of 8 unit cell LSMO took place under an oxygen pressure of 0.05 mbar, and it was *in situ* monitored by reflection high energy electron diffraction. TMO layers with a thickness of 40 nm were grown at a relatively higher oxygen pressure (0.4 mbar) on top of the LSMO layer. The reference single layers were prepared under the identical conditions. The structure of the samples was characterized using high-resolution x-ray diffraction (XRD) with a diffractometer (Smartlab, Rigaku, Japan) using Cu-Kα radiation. For the ultrathin (eight unit cells) LSMO single layer, synchrotron light (wavelength: 1.5386 Å) was used in the XRD measurements to achieve sufficient intensity. We characterized the magnetic properties of the bilayers and reference single layers using a superconducting quantum interference device (SQUID, Quantum Design, US) magnetometer.

1. Hwang, H. Y., Iwasa, Y., Kawasaki, M., Keimer, B., Nagaosa, N. & Tokura, Y. Emergent phenomena at oxide interfaces. *Nature Mater.* **11**, 103–113 (2012).
2. Chakhalian, J., Freeland, J. W., Habermeier, H.-U., Cristiani, G., Khaliullin, G., Veenendaal, M. van & Keimer, B. Orbital reconstruction and covalent bonding at an oxide interface. *Science* **318**, 1114–1117 (2007).
3. Reyren, N., Thiel, S., Caviglia, A. D., Fitting Kourkoutis, L., Hammerl, G., Richter, C., Schneider, C. W., Kopp, T., Rüetschi, A.-S., Jaccard, D., Gabay, M., Muller, D. A., Triscone, J.-M. & Mannhart, J. Superconducting interfaces between insulating oxides. *Science* **317**, 1196–1199 (2007).
4. You, L., Lu, C. L., Yang, P., Han, G. C., Wu, T., Luders, U., Prellier, W., Yao, K., Chen, L. & Wang, J. L. Uniaxial magnetic anisotropy in $La_{0.7}Sr_{0.3}MnO_3$ thin films induced by multiferroic $BiFeO_3$ with striped ferroelectric domains. *Adv. Mater.* **22**, 4964–4968 (2010).
5. Chakhalian, J., Freeland, J. W., Srajer, G., Strempfer, J., Khaliullin, G., Cezar, J. C., Charlton, T., Dalgliesh, R., Bernhard, C., Cristiani, G., Habermeier, H.-U. & Keimer, B. Magnetism at the interface between ferromagnetic and superconducting oxides. *Nat. Phys.* **2**, 244–248 (2006).
6. Kimura, T. Spiral magnets as magnetoelectrics. *Annu. Rev. Mater. Res.* **37**, 387–413 (2007).
7. Tokura, Y. & Seki, S. Multiferroics with spiral spin orders. *Adv. Mater.* **22**, 1554–1565 (2010).
8. Prellier, W., Singh, M. P. & Murugavel, P. The single-phase multiferroic oxides: from bulk to thin film. *J. Phys.: Condens. Matter* **17**, R803–R832 (2005).
9. Ramesh, R. & Spaldin, N. A. Multiferroics: progress and prospects in thin films. *Nature Mater.* **6**, 21–29 (2007).
10. Chen, Z. H., Luo, Z. L., Huang, C. W., Qi, Y. J., Yang, P., You, L., Hu, C. S., Wu, T., Wang, J. L., Gao, C., Sritharan, T. & Chen, L. Low–symmetry monoclinic phases and polarization rotation path mediated by epitaxial strain in multiferroic $BiFeO_3$ thin films. *Adv. Funct. Mater.* **21**, 133–138 (2011).
11. Cheng, C. J., Lu, C. L., Chen, Z. H., You, L., Chen, L., Wang, J. L. & Wu, T. Thickness-dependent magnetism and spin-glass behaviors in compressively strained $BiFeO_3$ thin films. *Appl. Phys. Lett.* **98**, 242502 (2011).
12. Zheng, H., Wang, J., Lofland, S. E., Ma, Z., Mohaddes-Ardabili, L., Zhao, T., Salamanca-Riba, L., Shinde, S. R., Ogale, S. B., Bai, F., Viehland, D., Jia, Y., Schlom, D. G., Wuttig, M., Roytburd, A. & Ramesh, R. Multiferroic $BaTiO_3$-$CoFe_2O_4$ nanostructures. *Science* **303**, 661–663 (2004).
13. Chu, Y.-H., Martin, L. W., Holcomb, M. B., Gajek, M., Han, S.-J., He, Q., Balke, N., Yang, C.-H., Lee, D., Hu, W., Zhan, Q., Yang, P.-L., Fraile-Rodríguez, A., Scholl, A., Wang, S. X. & Ramesh, R. Electric-field control of local ferromagnetism using a magnetoelectric multiferroic. *Nature Mater.* **7**, 478–482 (2008).
14. Yang, H., Jain, M., Suvorova, N. A., Zhou, H., Luo, H. M., Feldmann, D. M., Dowden, P. C., DePaula, R. F., Foltyn, S. R. & Jia, Q. X. Temperature-dependent leakage mechanisms of Pt/$BiFeO_3$/$SrRuO_3$ thin film capacitors. *Appl. Phys. Lett.* **91**, 072911 (2007).
15. Yamasaki, Y., Sagayama, H., Goto, T., Matsuura, M., Hirota, K., Arima, T. & Tokura, Y. Electric control of spin helicity in a magnetic ferroelectric. *Phys. Rev. Lett.* **98**, 147204 (2007).
16. Nogués, J. & Schuller, I. K. Exchange bias. *J. Magn. Magn. Mater.* **192**, 203–232 (1999).
17. Berkowitz, A. E. & Takano, K. Exchange anisotropy - a review. *J. Magn. Magn. Mater.* **200**, 552–570 (1999).
18. Kiwi, M. Exchange bias theory. *J. Magn. Magn. Mater.* **234**, 584–595 (2001).
19. Stamps, R. L. Mechanisms for exchange bias. *J. Phys. D-Appl. Phys.* **33**, R247–R268 (2000).
20. Nogués, J., Sort, J., Langlais, V., Skumryev, V., Suriñach, S., Muñoz, J. S. & Baró, M. D. Exchange bias in nanostructures. *Phys. Rep.* **422**, 65–117 (2005).
21. Dho, J., Qi, X., Kim, H., MacManus-Driscoll, J. L. & Blamire, M. G. Large electric polarization and exchange bias in multiferroic $BiFeO_3$. *Adv. Mater.* **18**, 1445–1448 (2006).
22. Dong, S., Yamauchi, K., Yunoki, S., Yu, R., Liang, S., Moreo, A., Liu, J.-M., Picozzi, S. & Dagotto, E. Exchange bias driven by the Dzyaloshinskii-Moriya interaction and ferroelectric polarization at G-type antiferromagnetic perovskites interfaces. *Phys. Rev. Lett.* **103**, 127201 (2009).
23. Cheng, Z. X., Zhao, H. Y., Du, Y., Kimura, H., Ozawa, K. & Wang, X. L. Exchange bias in multiferroic $BiFeO_3$ and $YMnO_3$ multilayers: one more parameter for magnetoelectric manipulation. *Scripta Materialia* **65**, 249–252 (2011).
24. Béa, H., Bibes, M., Ott, F., Dupé, B., Zhu, X.-H., Petit, S., Fusil, S., Deranlot, C., Bouzehouane, K. & Barthélémy, A. Mechanism of exchange bias with multiferroic $BiFeO_3$ epitaxial thin films. *Phys. Rev. Lett.* **100**, 017204 (2008).
25. Béa, H., Bibes, M., Cherifi, S., Nolting, F., Warot-Fonrose, B., Fusil, S., Herranz, G., Deranlot, C., Jacquet, E., Bouzehouane, K. & Barthélémy, A. Tunnel

magnetoresistance and robust room temperature exchange bias with multiferroic $BiFeO_3$ epitaxial thin films. *Appl. Phys. Lett.* **89**, 242114 (2006).
26. Martin, L. W., Chu, Y.-H., Holcomb, M. B., Huijiben, M., Yu, P., Han, S.-J., Lee, D., Wang, S. X. & Ramesh, R. Nanoscale control of exchange bias with $BiFeO_3$ thin films. *Nano Lett.* **8**, 2050–2055 (2008).
27. Wu, S. M., Cybart, S. A., Yu, P., Rossell, M. D., Zhang, J. X., Ramesh, R. & Dynes, R. C. Reversible electric control of exchange bias in a multiferroic field-effect device. *Nature Mater.* **9**, 756–761 (2010).
28. Malozemoff, A. P. Random-field model of exchange anisotropy at rough ferromagnetic-antiferromagnetic interfaces. *Phys. Rev. B* **35**, 3679–3682 (1987).
29. Koon, N. C. Calculation of exchange bias in thin films with ferromagnetic/antiferromagnetic interfaces. *Phys. Rev. Lett.* **78**, 4865–4868 (1997).
30. Tang, X. L., Zhang, H. W., Su, H., Jing, Y. L. & Zhong, Z. Y. Spin-transfer effect and independence of coercivity and exchange bias in a layered ferromagnet/antiferromagnet system. *Phys. Rev. B* **81**, 052401 (2010).
31. Schulthess, T. C. & Butler, W. H. Consequences of spin-flop coupling in exchange biased films. *Phys. Rev. Lett.* **81**, 4516–4519 (1998).
32. Leighton, C., Nogués, J., Jönsson-Åkerman, B. J. & Schuller, I. K. Coercivity enhancement in exchange biased systems driven by interfacial magnetic frustration. *Phys. Rev. Lett.* **84**, 3466–3469 (2000).
33. Panagiotopoulos, I., Christides, C., Pissas, M. & Niarchos, D. Exchange-biasing mechanism in $La_{2/3}Ca_{1/3}MnO_3/La_{1/3}Ca_{2/3}MnO_3$ multilayers. *Phys. Rev. B* **60**, 485–491 (1999).
34. Moutis, N., Christides, C., Panagiotopoulos, I. & Niarchos, D. Exchange-coupling properties of $La_{1-x}Ca_xMnO_3$ ferromagnetic/antiferromagnetic multilayers. *Phys. Rev. B* **64**, 094429 (2001).
35. Przyslupski, P., Komissarov, I., Paszkowic, W., Dluzewski, P., Minikayev, R. & Sawicki, M. Magnetic properties of $La_{0.67}Sr_{0.33}MnO_3/YBa_2Cu_3O_7$ superlattices. *Phys. Rev. B* **69**, 134428 (2004).
36. Ziese, M., Pippel, E., Nikulina, E., Arredondo, M. & Vrejoiu, I. Exchange coupling and exchange bias in $La_{0.7}Sr_{0.3}MnO_3$-$SrRuO_3$ superlattices. *Nanotechnology* **22**, 254025 (2011).
37. Ziese, M., Vrejoiu, I., Pippel, E., Nikulina, E. & Hesse, D. Magnetic properties of $Pr_{0.7}Ca_{0.3}MnO_3/SrRuO_3$ superlattices. *Appl. Phys. Lett.* **98**, 132504 (2011).
38. Ziese, M., Vrejoiu, I., Pippel, E., Esquinazi, P., Hesse, D., Etz, C., Henk, J., Ernst, A., Maznichenko, I. V., Hergert, W. & Mertig, I. Tailoring magnetic interlayer coupling in $La_{0.7}Sr_{0.3}MnO_3/SrRuO_3$ superlattices. *Phys. Rev. Lett.* **104**, 167203 (2010).
39. Kimura, T., Goto, T., Shintani, H., Ishizaka, K., Arima, T. & Tokura, Y. Magnetic control of ferroelectric polarization. *Nature* **426**, 55–58 (2003).
40. Lee, J.-H., Murugavel, P., Ryu, H., Lee, D., Jo, J. Y., Kim, J. W., Kim, H. J., Kim, K. H., Jo, Y., Jung, M.-H., Oh, Y. H., Kim, Y.-W., Yoon, J.-G., Chung, J.-S. & Noh, T. W. Epitaxial stabilization of a new multiferroic hexagonal phase of $TbMnO_3$ thin films. *Adv. Mater.* **18**, 3125–3129 (2006).
41. Xiang, H. J., Wei, S.-H., Whangbo, M.-H. & Da Silva, J. L. F. Spin-orbit coupling and ion displacements in multiferroic $TbMnO_3$. *Phys. Rev. Lett.* **101**, 037209 (2008).
42. Shuvaev, A. M., Travkin, V. D., Ivanov, V. Yu., Mukhin, A. A. & Pimenov, A. Evidence for electroactive excitation of the spin cycloid in $TbMnO_3$. *Phys. Rev. Lett.* **104**, 097202 (2010).
43. Kenzelmann, M., Harris, A. B., Jonas, S., Broholm, C., Schefer, J., Kim, S. B., Zhang, C. L., Cheong, S.-W., Vajk, O. P. & Lynn, J. W. Magnetic inversion symmetry breaking and ferroelectricity in $TbMnO_3$. *Phys. Rev. Lett.* **95**, 087206 (2005).
44. Voigt, J., Persson, J., Kim, J. W., Bihlmayer, G. & Brückel, Th. Strong coupling between the spin polarization of Mn and Tb in multiferroic $TbMnO_3$ determinded by x-ray resonance exchange scattering. *Phys. Rev. B* **76**, 104431 (2007).
45. Aliouane, N., Prokhnenko, O., Feyerherm, R., Mostovoy, M., Strempfer, J., Habicht, K., Rule, K. C., Dudzik, E., Wolter, A. U. B., Maljuk, A. & Argyriou, D. N. Magnetic order and ferroelectricity in $RMnO_3$ multiferroic manganites: coupling between R- and Mn-spins. *J. Phys.:Condens. Matter* **20**, 434215 (2008).
46. Kajimoto, R., Yoshizawa, H., Shintani, H., Kimura, T. & Tokura, Y. Magnetic structure of $TbMnO_3$ by neutron diffraction. *Phys. Rev. B* **70**, 012401 (2004).
47. Kimura, T. & Tokura, Y. Magnetoelectric phase control in a magnetic system showing cycloidal/conical spin order. *J. Phys.:Condens. Matter* **20**, 434204 (2008).
48. Hu, J. Microscopic origin of magnetoelectric coupling in noncollinear multiferroics. *Phys. Rev. Lett.* **100**, 077202 (2008).
49. Mochizuki, M. & Furukawa, N. Theory of magnetic switching of ferroelectricity in spiral magnets. *Phys. Rev. Lett.* **105**, 187601 (2010).
50. Rubi, D., Graaf, C. de, Daumont, C. J. M., Mannix, D., Broer, R. & Noheda, B. Ferromagnetism and increased iconicity in epitaxially grown $TbMnO_3$ films. *Phys. Rev. B* **79**, 014416 (2009).
51. Jehanathan, N., Lebedev, O., Gélard, I., Dubourdieu, C. & Tendeloo, G. V. Structure and defect characterization of multiferroic $ReMnO_3$ films and multilayers by TEM. *Nanotechnology* **21**, 075705 (2010).
52. Cui, Y. M., Tian, Y. F., Liu, W., Li, Y. F., Wang, R. M. & Wu, T. Interface-dependent rectifying $TbMnO_3$-based heterojunctions. *AIP Advances* **1**, 042129 (2011).
53. Cui, Y. M., Zhang, L. W., Wang, C. C., Xie, G. L., Chen, C. P. & Cao, B. S. Strain-assisted tunneling current through $TbMnO_3$/Nb-1 wt%-doped $SrTiO_3$ p-n junctions. *Appl. Phys. Lett.* **86**, 203501 (2005).
54. Mitsumata, C., Sakuma, A. & Fukamichi, K. Mechanism of the exchange-bias field in ferromagnetic and antiferromagnetic bilayers. *Phys. Rev. B* **68**, 014437 (2003).
55. Kirby, B. J., Kan, D., Luykx, A., Murakami, M., Kundaliya, D. & Takeuchi, I. Anomalous ferromagnetism in $TbMnO_3$ thin films. *J. Appl. Phys.* **105**, 07D917 (2009).
56. Daumont, C. J. M., Mannix, D., Venkatesan, S., Catalan, G., Rubi, D., Kooi, B. J., Hosson, J. Th M. De & Noheda, B. Epitaxial $TbMnO_3$ thin films on $SrTiO_3$ substrates: a structural study. *J. Phys.: Condens. Matter* **21**, 182001 (2009).
57. Hu, W. J., Zhou, G. H., Ren, W. J., Li, D. & Zhang, Z. D. Magnetic properties and unusual exchange coupling in self-organized $NdMnO_3/Mn_3O_4$ nanocomposite films. *J. Appl. Phys.* **110**, 013904 (2011).
58. Binder, K. & Young, A. P. Spin glasses: experimental facts, theoretical concepts, and open questions. *Rev. Mod. Phys.* **58**, 801–976 (1986).
59. Marti, X., Skumryev, V., Ferrater, C., García-Cuenca, M. V., Varela, M., Saánchez, F. & Fontcuberta, J. Emergence of ferromagnetism in antiferromagnetic $TbMnO_3$ by epitaxial strain. *Appl. Phys. Lett.* **96**, 222505 (2010).
60. Millis, A. J., Darling, T. & Migliori, A. Quantifying strain dependence in "colossal" magnetoresistance manganites. *J. Appl. Phys.* **83**, 1588–1591 (1998).
61. Tsui, F., Smoak, M. C., Nath, T. K. & Eom, C. B. Strain-dependent magnetic phase diagram of epitaxial $La_{0.67}Sr_{0.33}MnO_3$ thin films. *Appl. Phys. Lett.* **76**, 2421–2423 (2000).
62. Huijben, M., Martin, L. W., Chu, Y.-H., Holcomb, M. B., Yu, P., Rijnders, G., Blank, D. H. A. & Ramesh, R. Critical thickness and orbital ordering in ultrathin $La_{0.7}Sr_{0.3}MnO_3$ films. *Phys. Rev. B* **78**, 094413 (2008).
63. Dimitrov, D. V., Zhang, S., Xiao, J. Q., Hadjipanayis, G. C. & Prados, C. Effect of exchange interactions at antiferromagnetic/ferromagnetic interfaces on exchange bias and coercivity. *Phys. Rev. B* **58**, 12090–12594 (1998).
64. Fina, I., Fàbrega, L., Martí, X., Sánchez, F. & Fontcuberta, J. Chiral domains in cycloidal multiferroic thin films: switching and memory effects. *Phys. Rev. Lett.* **107**, 257601 (2011).
65. Chu, Y.-H., Zhan, Q., Martin, L. W., Cruz, M. P., Yang, P.-L., Pabst, G. W., Zavaliche, F., Yang, S.-Y., Zhang, J.-X., Chen, L.-Q., Schlom, D. G., Lin, I.-N., Wu, T.-B. & Ramesh, R. Nanoscale domain control in multiferroic $BiFeO_3$ thin films. *Adv. Mater.* **18**, 2307–2311 (2006).

Acknowledgments

The authors acknowledge the support from the National Research Foundation of Singapore.

Author contributions

Y.F.T. and T.W. conceived and designed the experiments. Y.F.T., J.F.D., W.N.L., Z.H.C., A.D., M.H. and W.J.H. carried out the experiments. Y.F.T. and T.W. wrote the paper. All authors discussed the results and commented on the manuscript.

Additional information

Competing financial interests: The authors declare no competing financial interests.

How to cite this article: Tian, Y.F. *et al*. Anomalous exchange bias at collinear/noncollinear spin interface. *Sci. Rep.* **3**, 1094; DOI:10.1038/srep01094 (2013).